We are IntechOpen, the world's leading publisher of Open Access books Built by scientists, for scientists

4,800
Open access books available

122,000
International authors and editors

135M
Downloads

Our authors are among the

154
Countries delivered to

TOP 1%
most cited scientists

12.2%
Contributors from top 500 universities

WEB OF SCIENCE™

Selection of our books indexed in the Book Citation Index in Web of Science™ Core Collection (BKCI)

Interested in publishing with us?
Contact book.department@intechopen.com

Numbers displayed above are based on latest data collected.
For more information visit www.intechopen.com

16

A Dual-Mode Wide-Band Bandpass Filter Using the Microstrip Loop Resonator with Tuning Stubs

Jessada Konpang
Rajamangala University of Technology Krungthep
Thailand

1. Introduction

The broadband wireless access (BWA) is an important issue in current developments of the modern wireless communication system. To meet this trend, the bandpass filters with relatively wide bandwidth are frequently required in the RF front ends. In microwave communication systems, the bandpass filter is an essential component, which is usually used in both receivers and transmitters. Thus, the quality of bandpass filers is extremely important. Planar filters are currently a popular structure because they can be fabricated using printed circuit technology and are suitable for commercial applications due to their small size and lower fabrication cost (D.M. Pozar, 1998). Therefore, how to design a bandpass filter at low cost and with high performance is currently of great interest. Microstrip bandpass filters can be easily mounted on a dielectric substrate and can provide a more flexible design of the circuit layout. The dual-mode resonators filter have been known for years. The compact high performance microwave bandpass filters are highly desirable in the wireless communications systems. Consequently, the dual-mode filters have been used widely for the system because of their advantages such as small size, light weight, low loss and high selectivity. Many authors (Hsieh & Chang, 2001, 2003), (Konpang, 2003) and (Chen et al., 2005) have proposed the wide-band bandpass filters using dual-mode ring resonators with tuning stubs but the configurations still occupy a large circuit area, which is not suitable for wireless communication systems where the miniaturization is an important factor. Therefore, it is desirable to develop new types of dual-mode microstrip resonators not only for offering alternative designs, but also for miniaturizing filters. On the other hand, the modern wireless communication systems require the bandpass filters having effective out-of-band spurious rejection and good in-band performance. The resonators with reasonable spurious are required to meet the out-of-band requirements. The microstrip open-loop resonators have a wide stopband resulting from the dispersion effect and the slow-wave effect (Hong & Lancaster, 1997) and (Görür, 2002).
In this book, a dual-mode wide-band bandpass filter using the microstrip loop resonators with tuning stubs is proposed. Basic concepts and design equations for microstrip lines introduced in section 2. The bandpass filter is based on the bandstop filter employing direct-

connected feed lines on the orthogonal of the microstrip loop resonators. The introduction of two tuning open stubs connecting opposite to the ports widens the passband and sharpens the stopbands. Then, a dual-mode can be used to improve the narrow stopbands for lower side band and higher sideband. The design descriptions dual-mode wide-band bandpass filter are discussed in section 3.

2. Transmission lines

Basic concepts and design equations for microstrip lines, dual-mode wide-band bandpass filter using the microstrip loop resonator with tuning stubs are briefly described.

2.1 Microstrip lines

2.1.1 Microstrip structure

The general structure of a microstrip is illustrated in Figure 1. A conducting strip (microstrip line) with a width w and a thickness t is on the top of a dielectric substrate that has a relative dielectric constant ε_r and a thickness h, and the bottom of the substrate is a ground (conducting) plane.

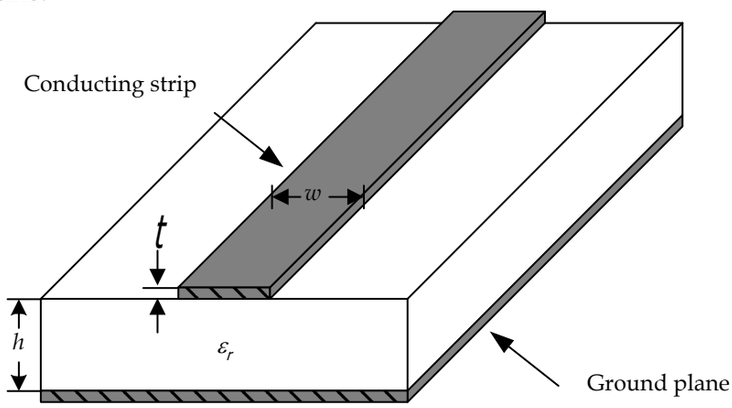

Fig. 1. General microstrip structure

2.1.2 Waves in microstrips

The fields in the microstrip extend within two media-air above and dielectric below so that the structure is inhomogeneous. Due to this inhomogeneous nature, the microstrip does not support a pure TEM wave. This is because that a pure TEM wave has only transverse components, and its propagation velocity depends only on the material properties, namely the permittivity ε and the permeability μ. However, with the presence of the two guided-wave media (the dielectric substrate and the air), the waves in a microstrip line will have no vanished longitudinal components of electric and magnetic fields, and their propagation velocities will depend not only on the material properties, but also on the physical dimensions of the microstrip.

2.1.3 Quasi-TEM approximation

When the longitudinal components of the fields for the dominant mode of a microstrip line remain very much smaller than the transverse components, they may be neglected. In this

case, the dominant mode then behaves like a TEM mode, and the TEM transmission line theory is applicable for the microstrip line as well. This is called the quasi-TEM approximation and it is valid over most of the operating frequency ranges of microstrip.

2.1.4 Effective dielectric constant and characteristic impedance

In the quasi-TEM approximation, a homogeneous dielectric material with an effective dielectric permittivity replaces the inhomogeneous dielectric-air media of microstrip. Transmission characteristics of microstrips are described by two parameters, namely the effective dielectric constant ε_{re} and characteristic impedance Z_c, which may then be obtained by quasistatic analysis. In quasi-static analysis, the fundamental mode of wave propagation in a microstrip is assumed to be pure TEM. The above two parameters of microstrips are then determined from the values of two capacitances as follows

$$\varepsilon_{re} = \frac{C_d}{C_a}$$
$$Z_c = \frac{1}{c\sqrt{C_a C_d}} \tag{1}$$

in which C_d is the capacitance per unit length with the dielectric substrate present, C_a is the capacitance per unit length with the dielectric substrate replaced by air, and c is the velocity of electromagnetic waves in free space $(c \approx 3.0 \times 10^8 m/s)$.

For very thin conductors (i.e., $t \to 0$), the closed-form expressions that provide an accuracy better than one percent are given as follows (Hong & Lancaster, 2001).

For $w/h \le 1$:

$$\varepsilon_{re} = \frac{\varepsilon_r + 1}{2} + \frac{\varepsilon_r - 1}{2}\left\{\left(1 + 12\frac{h}{w}\right)^{-0.5} + 0.04\left(1 - \frac{w}{h}\right)^2\right\} \tag{2a}$$

$$Z_c = \frac{\eta}{2\pi\sqrt{\varepsilon_{re}}}\ln\left(\frac{8h}{w} + 0.25\frac{w}{h}\right) \tag{2b}$$

where $\eta = 120\pi$ ohms is the wave impedance in free space.

For $w/h \ge 1$:

$$\varepsilon_{re} = \frac{\varepsilon_r + 1}{2} + \frac{\varepsilon_r - 1}{2}\left(1 + 12\frac{h}{w}\right)^{-0.5} \tag{3a}$$

$$Z_c = \frac{\eta}{\sqrt{\varepsilon_{re}}}\left\{\frac{w}{h} + 1.393 + 0.677\ln\left(\frac{w}{h} + 1.444\right)\right\}^{-1} \tag{3b}$$

Accurate expression for the effective dielectric constant is

$$\varepsilon_{re} = \frac{\varepsilon_r + 1}{2} + \frac{\varepsilon_r - 1}{2}\left(1 + \frac{10}{u}\right)^{-ab} \tag{4}$$

Where $u = w/h$, and

$$a = 1 + \frac{1}{49}\ln\left(\frac{u^4 + \left(\frac{u}{52}\right)^2}{u^4 + 0.432}\right) + \frac{1}{18.7}\ln\left(1 + \left(\frac{u}{18.1}\right)^3\right)$$

$$b = 0.564\left(\frac{\varepsilon_r - 0.9}{\varepsilon_r + 3}\right)^{0.053}$$

The accuracy of this model is better than 0.2% for $\varepsilon_r \le 128$ and $0.01 \le u \le 100$.
The more accurate expression for the characteristic impedance is

$$Z_c = \frac{\eta}{2\pi\sqrt{\varepsilon_{re}}}\ln\left[\frac{F}{u} + \sqrt{1 + \left(\frac{2}{u}\right)^2}\right] \tag{5}$$

where $u = w/h$, $\eta = 120\pi$ ohms, and

$$F = 6 + (2\pi - 6)\exp\left[-\left(\frac{30.666}{u}\right)^{0.7528}\right]$$

The accuracy for $Z_c\sqrt{\varepsilon_{re}}$ is better than 0.01% for $u \le 1$ and 0.03% for $u \le 1000$.

2.1.5 Guided wavelength, propagation constant, phase velocity, and electrical length

Once the effective dielectric constant of a microstrip is determined, the guided wavelength of the quasi-TEM mode of microstrip is given by

$$\lambda_g = \frac{\lambda_0}{\sqrt{\varepsilon_{re}}} \tag{6a}$$

where λ_0 is the free space wavelength at operation frequency *f*. More conveniently, where the frequency is given in gigahertz (GHz), the guided wavelength can be evaluated directly in millimeters as follows:

$$\lambda_g = \frac{300}{f(GHz)\sqrt{\varepsilon_{re}}} mm \tag{6b}$$

The associated propagation constant *(β)* and phase velocity (v_p) can be determined by

$$\beta = \frac{2\pi}{\lambda_g} \tag{7}$$

$$v_p = \frac{w}{\beta} = \frac{c}{\sqrt{\varepsilon_{re}}} \tag{8}$$

where c is the velocity of light $(c \approx 3.0 \times 10^8 m/s)$ in free space.
The electrical length *(θ)* for a given physical length (*l)* of the microstrip is defined by

$$\theta = \beta l \tag{9}$$

Therefore, $\theta = \pi/2$ when $l = \lambda_g/4$, and $\theta = \pi$ when $l = \lambda_g/2$. These so-called quarterwavelength and half-wavelength microstrip lines are important for design of microstrip filters.

2.1.6 Synthesis of *w/h*

Approximate expressions for w/h in terms of Z_c and ε_r are available.
For $w/h \leq 2$

$$\frac{w}{h} = \frac{8\exp(A)}{\exp(2A) - 2} \tag{10}$$

with

$$A = \frac{Z_c}{60}\left\{\frac{\varepsilon_r + 1}{2}\right\}^{0.5} + \frac{\varepsilon_r - 1}{\varepsilon_r + 1}\left\{0.23 + \frac{0.11}{\varepsilon_r}\right\} \tag{11}$$

and for $w/h \geq 2$

$$\frac{w}{h} = \frac{2}{\pi}\left\{(B-1) - \ln(2B-1) + \frac{\varepsilon_r - 1}{2\varepsilon_r}\left[\ln(B-1) + 0.39 - \frac{0.61}{\varepsilon_r}\right]\right\} \tag{11}$$

with

$$B = \frac{60\pi^2}{Z_c\sqrt{\varepsilon_r}}$$

These expressions also provide accuracy better than one percent. If more accurate values are needed, an iterative or optimization process based on the more accurate analysis models described previously can be employed.

2.1.7 Effect of strip thickness

So far we have not considered the effect of conducting strip thickness t (as referring to Figure 1). The thickness t is usually very small when the microstrip line is realized by conducting thin films; therefore, its effect may quite often be neglected. Nevertheless, its effect on the characteristic impedance and effective dielectric constant may be included.
For $w/h \leq 1$:

$$Z_c(t) = \frac{\eta}{2\pi\sqrt{\varepsilon_{re}}}\ln\left\{\frac{8}{w_e(t)/h} + 0.25\frac{w_e(t)}{h}\right\} \tag{12a}$$

For $w/h \geq 1$:

$$Z_c(t) = \frac{\eta}{\sqrt{\varepsilon_{re}}}\left\{\frac{w_e(t)}{h} + 1.393 + 0.667\ln\left(\frac{w_e(t)}{h} + 1.444\right)\right\}^{-1} \tag{12b}$$

where

$$\frac{w_e(t)}{h} = \begin{cases} \dfrac{w}{h} + \dfrac{1.25}{\pi}\dfrac{t}{h}\left(1 + \ln\dfrac{4\pi w}{t}\right) & (w/h \le 0.5\pi) \\ \dfrac{w}{h} + \dfrac{1.25}{\pi}\dfrac{t}{h}\left(1 + \ln\dfrac{2h}{t}\right) & (w/h \ge 0.5\pi) \end{cases} \tag{13a}$$

$$\varepsilon_{re}(t) = \varepsilon_{re} - \frac{\varepsilon_r - 1}{4.6}\frac{t/h}{\sqrt{w/h}} \tag{13b}$$

In the above expressions, ε_{re} is the effective dielectric constant for $t = 0$. It can be observed that the effect of strip thickness on both the characteristic impedance and effective dielectric constant is insignificant for small values of t/h. However, the effect of strip thickness is significant for conductor loss of the microstrip line.

2.1.8 Dispersion in microstrip

Generally speaking, there is dispersion in microstrips; namely, its phase velocity is not a constant but depends on frequency. It follows that its effective dielectric constant ε_{re} is a function of frequency and can in general be defined as the frequencydependent effective dielectric constant $\varepsilon_{re}(f)$. The previous expressions for ε_{re} are obtained based on the quasi-TEM or quasistatic approximation, and therefore are rigorous only with DC. At low microwave frequencies, these expressions provide a good approximation. To take into account the effect of dispersion, the formula of $\varepsilon_{re}(f)$ is given as follows (Hong & Lancaster, 2001).

$$\varepsilon_{re}(f) = \varepsilon_r - \frac{\varepsilon_r - \varepsilon_{re}}{1 + \left(f / f_{50}\right)^m} \tag{14}$$

where

$$f_{50} = \frac{f_{TM_0}}{0.75 + \left(0.75 - 0.332\varepsilon_r^{-1.73}\right)w/h} \tag{15a}$$

$$f_{TM_0} = \frac{c}{2\pi h\sqrt{\varepsilon_r - \varepsilon_{re}}}\tan^{-1}\left(\varepsilon_r\frac{\sqrt{\varepsilon_{re} - 1}}{\varepsilon_r - \varepsilon_{re}}\right) \tag{15b}$$

$$m = m_0 m_c \le 2.32 \tag{16a}$$

$$m_0 = 1 + \frac{1}{1 + \sqrt{w/h}} + 0.32\left(\frac{1}{1 + \sqrt{w/h}}\right)^3 \tag{16b}$$

$$m_c = \begin{cases} 1 + \dfrac{1.4}{1 + w/h}\left\{0.15 - 0.235\exp\left(\dfrac{-0.45f}{f_{50}}\right)\right\} & \text{for } w/h \le 0.7 \\ 1 & \text{for } w/h \ge 0.7 \end{cases} \tag{16c}$$

where c is the velocity of light in free space, and whenever the product $m_0 m_c$ is greater than 2.32, the parameter m is chosen equal to 2.32. The dispersion model shows that the $\varepsilon_{re}(f)$ increases with frequency, and $\varepsilon_{re}(f) \to \varepsilon_r$ as $f \to \infty$. The accuracy is estimated to be within 0.6% for $0.1 \le w/h \le 10$, $1 \le \varepsilon_r \le 128$ and for any value of h/λ_0.
The effect of dispersion on the characteristic impedance may be estimated by

$$Z_c(f) = Z_c \frac{\varepsilon_{re}(f) - 1}{\varepsilon_{re} - 1}\sqrt{\frac{\varepsilon_{re}}{\varepsilon_{re}(f)}} \tag{17}$$

where Z_c is the quasi-static value of characteristic impedance obtained earlier.

2.2 Microstrip discontinuities

Microstrip discontinuities commonly encountered in the layout of practical filters include junctions, bends and open stubs. Generally speaking, the effects of discontinuities can be more accurately modeled and taken into account in the filter designs with full-wave electromagnetic (EM) simulations.

2.2.1 Junction

The junction is used when we wish to split a signal into another paths. The asymmetrical microstrip line T junction is indicated in Figure 2.

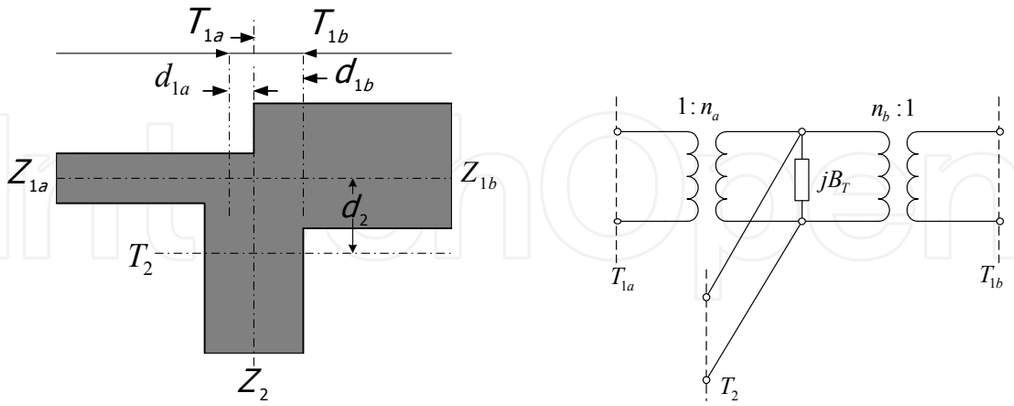

Fig. 2. Asymmetric microstrip line T junction and Model
The equations for a symmetric T junction to model the asymmetric junction. The equations are

$$\frac{d_{1a}}{D_2} = 0.055\left[1 - 2\frac{Z_{1a}}{Z_2}\left(\frac{f}{f_{p1}}\right)^2\right]\frac{Z_{1a}}{Z_2} \tag{18}$$

$$\frac{d_{1b}}{D_2} = 0.055\left[1 - 2\frac{Z_{1b}}{Z_2}\left(\frac{f}{f_{p1}}\right)^2\right]\frac{Z_{1b}}{Z_2} \tag{19}$$

$$\begin{aligned}\frac{d_2}{D_1} = 0.5 - \Bigg[&0.05 + 0.7\exp\left(-1.6\frac{\sqrt{Z_{1a}Z_{1b}}}{Z_2}\right)\\ &+ 0.25\frac{\sqrt{Z_{1a}Z_{1b}}}{Z_2}\left(\frac{f}{f_{p1}}\right)^2 - 0.17\ln\frac{\sqrt{Z_{1a}Z_{1b}}}{Z_2}\Bigg]\frac{\sqrt{Z_{1a}Z_{1b}}}{Z_2}\end{aligned} \tag{20}$$

$$n_a{}^2 = 1 - \pi\left(\frac{f}{f_{p1}}\right)^2\left[\frac{1}{12}\left(\frac{Z_{1a}{}^2}{Z_2}\right) + \left(0.5 - \frac{d_2}{D_1}\right)^2\right] \tag{21}$$

$$n_b{}^2 = 1 - \pi\left(\frac{f}{f_{p1}}\right)^2\left[\frac{1}{12}\left(\frac{Z_{1b}{}^2}{Z_2}\right) + \left(0.5 - \frac{d_2}{D_1}\right)^2\right] \tag{22}$$

$$\begin{aligned}\frac{B_T}{Y_2}\frac{\lambda_1}{D_1} = 5.5\frac{\varepsilon_r + 2}{\varepsilon_r}\Bigg[&1 + 0.9\ln\frac{\sqrt{Z_{1a}Z_{1b}}}{Z_2} + 4.5\frac{\sqrt{Z_{1a}Z_{1b}}}{Z_2}\left(\frac{f}{f_{p1}}\right)^2\\ &- 4.4\exp\left(-1.3\frac{\sqrt{Z_{1a}Z_{1b}}}{Z_2}\right) - 20\left(\frac{Z_2}{\eta_0}\right)^2\Bigg]n^{-2}\frac{d_1}{D_2}\end{aligned} \tag{23}$$

where

$$D = \frac{\eta_0 h}{\left(\sqrt{\varepsilon_{re}}Z_c\right)} \tag{24}$$

$$f_p(GHz) = \frac{0.4Z_c}{h} \tag{25}$$

2.2.2 Bends

Right-angle bend and mitered bend of microstrips may be modeled by and equivalent T-network, as shown in Figure 3. (Kupta et al., 1996) have given closed-form expressions for evaluation of capacitance and inductance:

$$C = 0.001h\left[(10.35\varepsilon_r + 2.5)\left(\frac{w}{h}\right)^2 + (2.6\varepsilon_r + 5.64)\left(\frac{w}{h}\right)\right]\ p\text{F} \tag{26}$$

$$L = 0.22h\left\{1 - 1.35\exp\left[-0.18\left(\frac{w}{h}\right)^{1.39}\right]\right\} \text{ nH} \tag{27}$$

for the microstrip mitered bend, and as

$$C = 0.001h\left[(3.93\varepsilon_r + 0.62)\left(\frac{w}{h}\right)^2 + (7.6\varepsilon_r + 3.8)\left(\frac{w}{h}\right)\right] p\text{F} \tag{28}$$

$$L = 0.44h\left\{1 - 1.062\exp\left[-0.177\left(\frac{w}{h}\right)^{0.947}\right]\right\} \text{ nH} \tag{29}$$

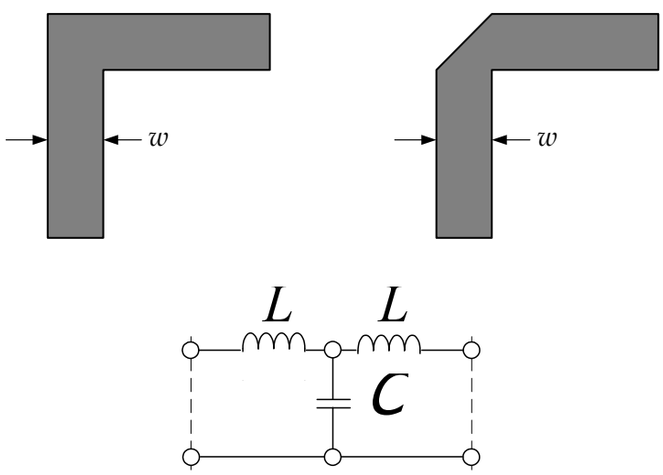

Fig. 3. Right-angle bend, mitered bend and model

2.2.3 Open stub

According to the transmission line theory, the input admittance of an open circuited transmission line having a characteristic admittance $Y_c = 1/Z_c$ and propagation constant $\beta = 2\pi/\lambda_g$ is give by

$$Y_t = jY_c \tan\left(\frac{2\pi}{\lambda_g} l\right) \tag{30}$$

Where l is the length of the stub. If $l < \lambda_g/4$ this input admittance is capacitive. The input admittance may be approximated by

$$Y_t \approx jY_c\left(\frac{2\pi}{\lambda_g} l\right) = j\omega\left(\frac{Y_c l}{v_p}\right) \tag{31}$$

Where v_p is the phase velocity of propagation in the stub. It is now clearer that such a open circuited stub is equivalent to a shunt capacitance $C = Y_c l / v_p$, as indicated in Figure 4.

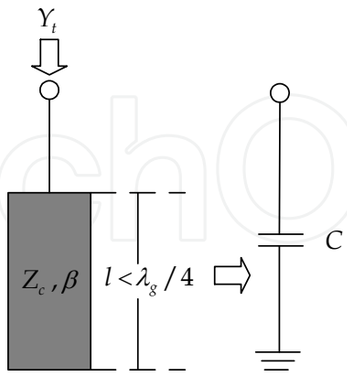

Fig. 4. Open circuit stub and Model

At the open end of a microstrip line with a width of w , the fields do not stop abruptly but extend slightly further due to the effect of the fringing field. This effect can be modeled either with an equivalent shunt capacitance C_p or with an equivalent length of transmission line

$$l_{open} = \frac{cZ_c C_p}{\sqrt{\varepsilon_{re}}} \tag{32}$$

Where c is the light velocity in free space. A closed-form expression for l_{open} / h is given by

$$\frac{l_{open}}{h} = \frac{\xi_1 \xi_3 \xi_5}{\xi_4} \tag{33}$$

where

$$\xi_1 = 0.434907 \frac{\varepsilon_{re}^{0.81} + 0.26(w/h)^{0.8544} + 0.236}{\varepsilon_{re}^{0.81} - 0.189(w/h)^{0.8544} + 0.87} \tag{34}$$

$$\xi_2 = 1 + \frac{(w/h)^{0.371}}{2.35\varepsilon_r + 1} \tag{35}$$

$$\xi_3 = 1 + \frac{0.5274 \arctan\left[0.084(w/h)^{1.9413/\xi_2}\right]}{\varepsilon_{re}^{0.9236}} \tag{36}$$

$$\xi_4 = 1 + 0.0377 \arctan\left[0.067(w/h)^{1.456}\right]\left\{6 - 5\exp\left[0.036(1-\varepsilon_r)\right]\right\} \tag{37}$$

$$\xi_5 = 1 - 0.218\exp(-7.5w/h) \tag{38}$$

The accuracy is better than 0.2% for the range of $0.01 \le w/h \le 100$ and $\varepsilon_r \le 128$.

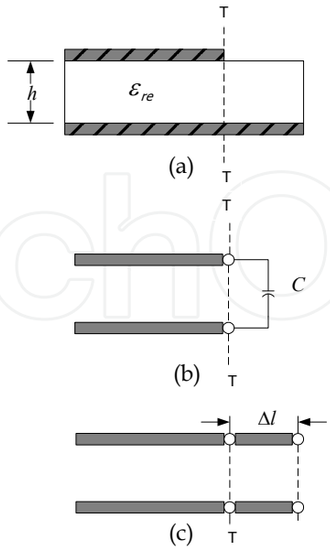

Fig. 5. (a) Microstrip open-end discontinuity (b) equivalent capacitance representation, and (c) equivalent line length representation

3. Dual-mode wide-band bandpass filter design

The bandpass filter is based on the bandstop filter employing direct-connected feed lines on the orthogonal of the microstrip loop resonators. The introduction of two tuning open stubs connecting opposite to the ports widens the passband and sharpens the stopbands. Then, a dual-mode can be used to improve the narrow stopbands for lower side band and higher sideband.

3.1 Bandstop characteristics

3.1.1 Bandstop filter (Type A)

The first bandpass filter is based on the bandstop filter employing direct-connected feed lines on the orthogonal of the microstrip loop resonator (Konpang et al., (2007). The microstrip loop resonator with direct-connected feed lines on the orthogonal depicted in Fig. 6 is a bandstop configuration. The resonator consists of four identical branches with attached to an outer corner of the square loop. The bandstop filter is designed at fundamental resonant frequency f_0 = 2.45 GHz and fabricated on a RT/Duroid substrate having a thickness h = 1.27 mm with relative dielectric constant ε_r = 6.15. The filter was designed and simulated by IE3D program. The dimensions of the loop are l_f = 8 mm, s = 0.715 mm, w_1 = 1.85 mm, w_2 = 0.75 mm, w_3 = 1.35 mm and a = 9.3 mm.

The equivalent microstrip loop circuit as shown in Fig. 7 is divided into input and output ports forming a shunt circuit denoted by the upper and lower parts, respectively. The capacitance jB_{T1} is the T-junction effect between the feed line and the microstrip loop resonator (Hsieh & Chang, 2003). The capacitance jB_{T2} is the junction effect between the

loop resonator with each branch. The analysis of the characteristic of the microstrip loop resonators is performed by IE3D program. Fig.8 presents the simulation results of the microstrip loop using direct-connect orthogonal feed lines, the frequency response exhibits bandstop behaviours.

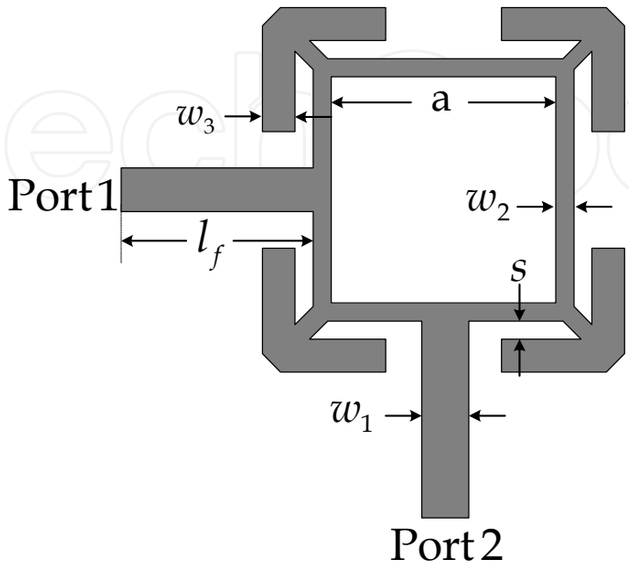

Fig. 6. Microstrip loop resonator using direct-connected orthogonal feeders (Type A)

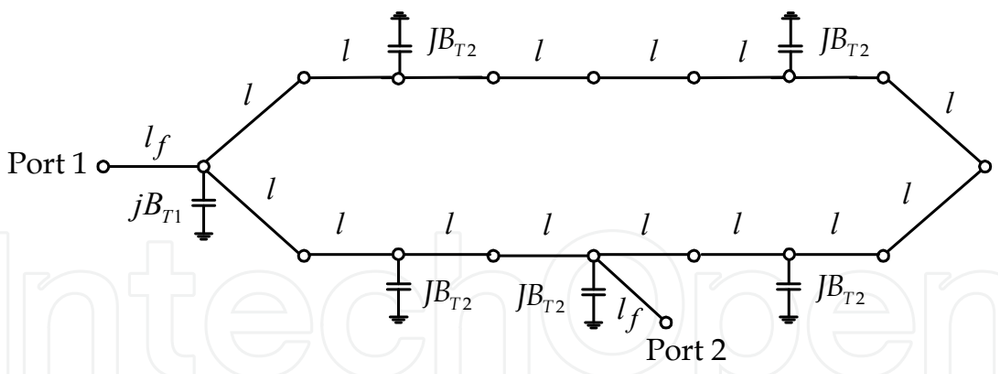

Fig. 7. Equivalent circuit of the microstrip loop resonator using direct-connected orthogonal feed lines

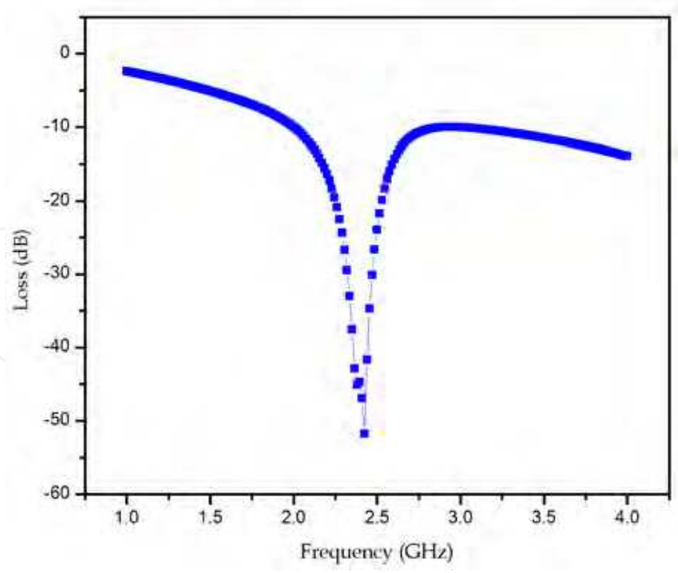

Fig. 8. Simulation results of the microstrip loop resonator using direct-connected orthogonal feed lines

3.1.2 Bandstop filter (Type B)

The second bandpass filter is based on the bandstop filter employing direct-connected feed lines on the orthogonal of the microstrip loop resonator (J. Konpang, 2008). The microstrip loop resonator with direct-connected feed lines on the orthogonal depicted in Fig.9 is a bandstop configuration. The resonator consists of four identical branches with a small square patch attached to an inner corner of the square loop.

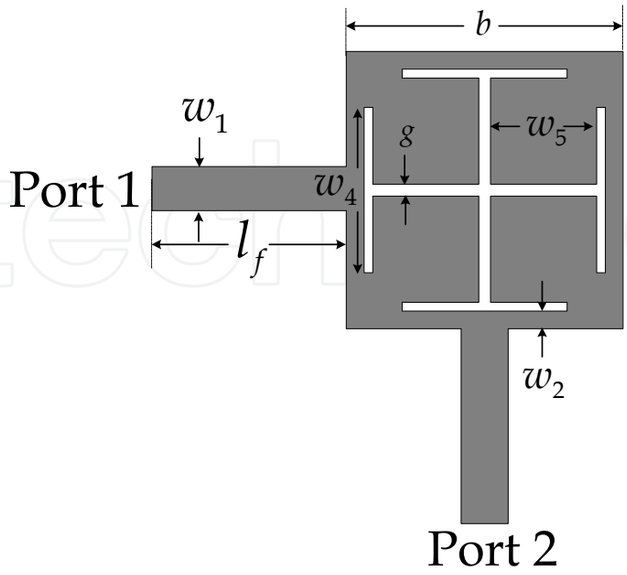

Fig. 9. Microstrip loop resonator using direct-connected orthogonal feeders (Type B)

The bandstop filters is designed at fundamental resonant frequency f_0 = 2.45 GHz and fabricated on a RT/Duroid substrate having a thickness h = 1.27 mm with relative dielectric constant ε_r = 6.15. The filter was designed and simulated by IE3D program. The dimensions of the loop are l_f = 8 mm, w_1 = 1.85 mm, w_2 = 0.75 mm, w_4 = 6.8 mm, w_5 = 4.4 mm, g = 0.4 mm and b = 11.5 mm.

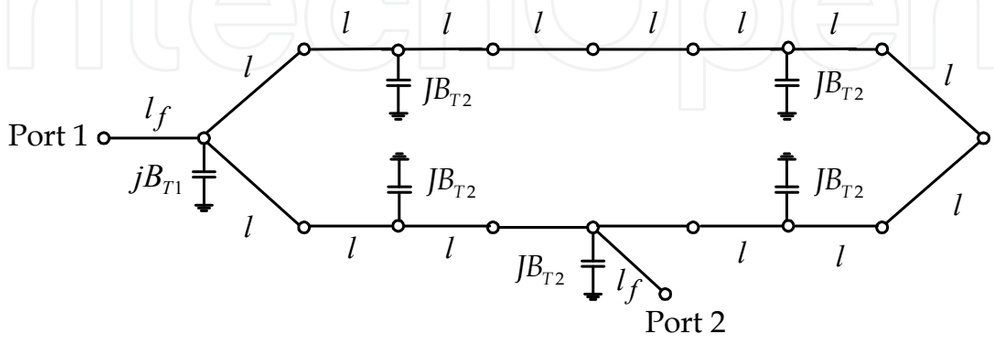

Fig. 10. Equivalent circuit of the microstrip loop resonator using direct-connected orthogonal feed lines

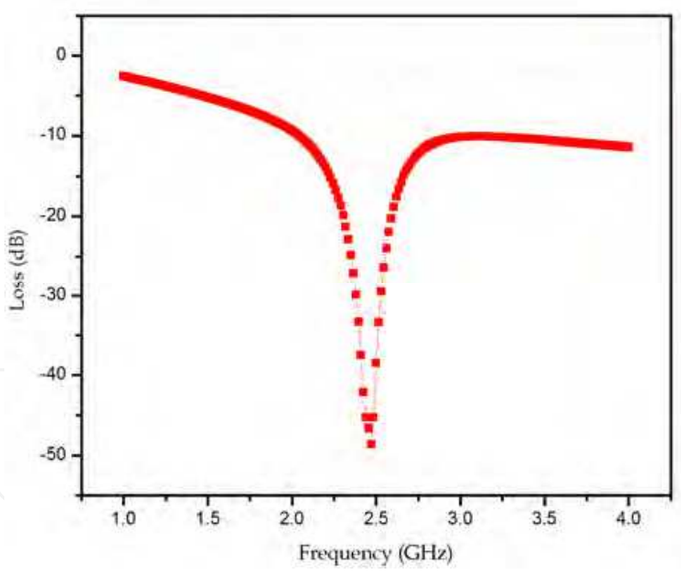

Fig. 11. Simulation results of the microstrip loop resonator using direct-connected orthogonal feed lines

The equivalent microstrip loop circuit is shown in Fig.10 is divided into input and output ports forming a shunt circuit denoted by the upper and lower parts, respectively. The capacitance jB_{T1} is the T-junction effect between the feed line and the microstrip loop resonator (Hsieh & Chang, 2003). The capacitance jB_{T2} is the junction effect between the loop resonator with each branch. The analysis of the characteristic of the microstrip loop

resonators is performed by IE3D program. Fig.11 presents the simulation results of the microstrip loop using direct-connect orthogonal feed lines. The frequency response exhibits bandstop behaviours.

3.2 Two tuning stubs for a single-mode bandpass filter

3.2.1 Single-mode bandpass filter (Type A)

Based on bandstop filter, The first resonator is modified by adding two tuning stubs connecting opposite to the ports. The resonator (Type A) with tuning stubs is shown in Fig. 12. The length of tuning opened-stub is $l_t = \lambda_g / 4$.

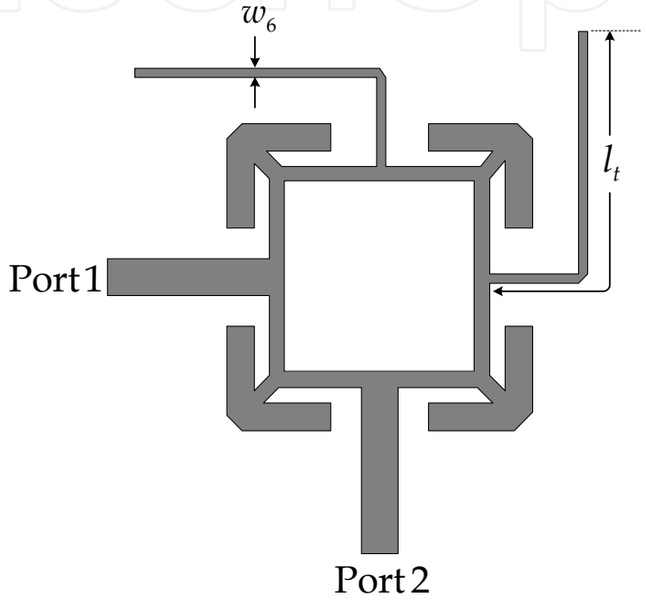

Fig. 12. Structure of two tuning stubs for single-mode (Type A)

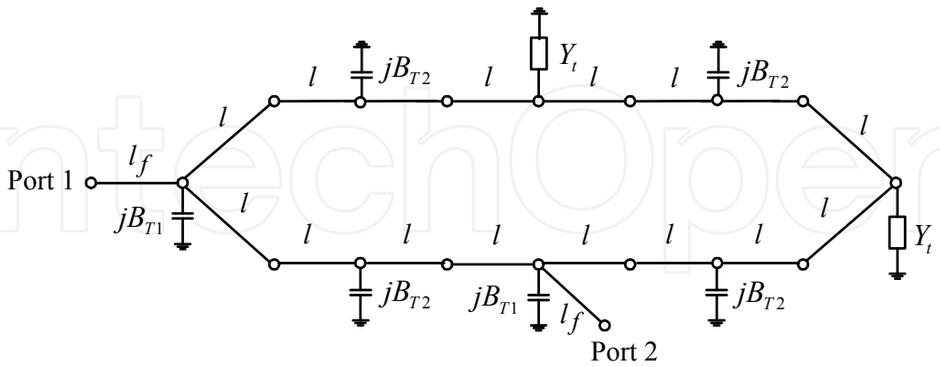

Fig. 13. Equivalent circuit of a microstrip loop resonator with tuning stubs

The equivalent circuit of resonator with tuning stubs is shown in Fig. 13. Y_t is the admittance reflecting into the stubs Y_t can be expressed by

$$Y_t = y_o \tanh(\gamma lt + l_{open}) + jB_{T3} \tag{39}$$

where y_o is the characteristic admittance of the stub, γ is the complex propagation constant, l_{open} is the equivalent open effect length and jB_{T3} is the capacitance of the T-junction between the microstrip loop with stubs l_t .

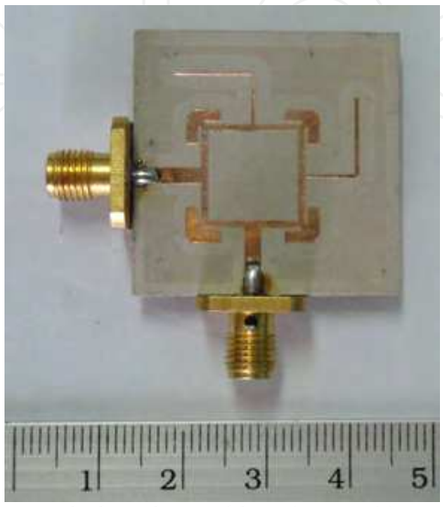

Fig. 14. Photograph of a single-mode bandpass filter (Type A)

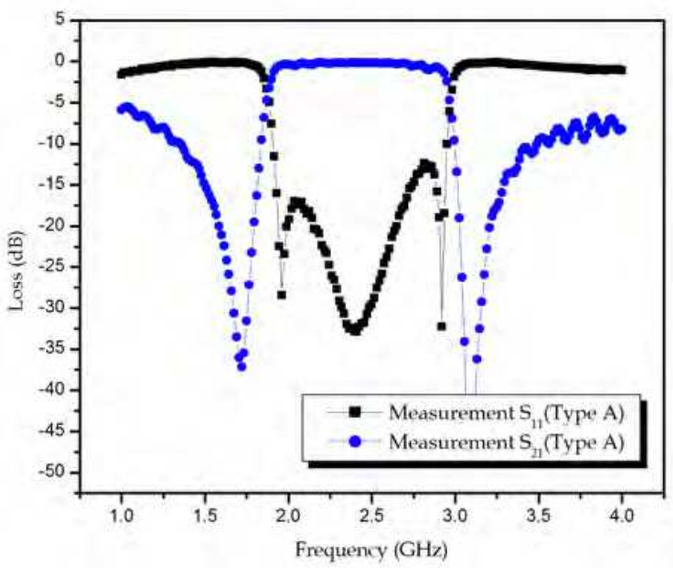

Fig. 15. Measurement for single-mode bandpass filter

The implemented of single-mode resonators filter is pictured in Fig. 14. The measurement results of the microstrip loop with tuning stubs of l_t = 16.25 mm, $w_6 = 0.4$ mm . The frequency response of the filter is portrayed in Fig. 15. The introduction of two tuning stubs connecting opposite to the ports widens the passband and sharpens the stopbands. The

single-mode filter exhibits the 3-dB fractional bandwidth of the filter is 37%, the insertion loss better than 0.26 dB and return loss greater than 12.6 dB in the passband.
In fact, this approach can be interpreted as using two stopbands induced by two tuning stubs in conjunction with the wide passband. In some cases, an undesired passband below the main passband may require a high passband section to be employed in conjunction with this proposing approach.

3.2.2 Single-mode bandpass filter (Type B)

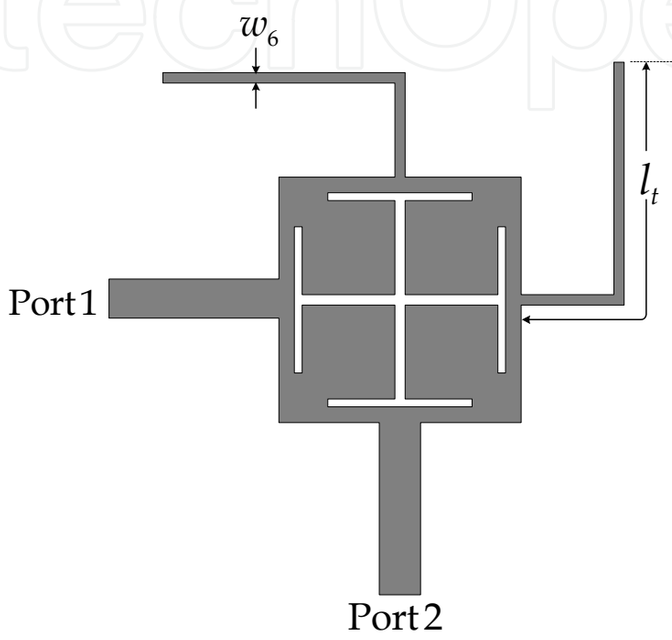

Fig. 16. Structure of two tuning stubs for single-mode (Type B)

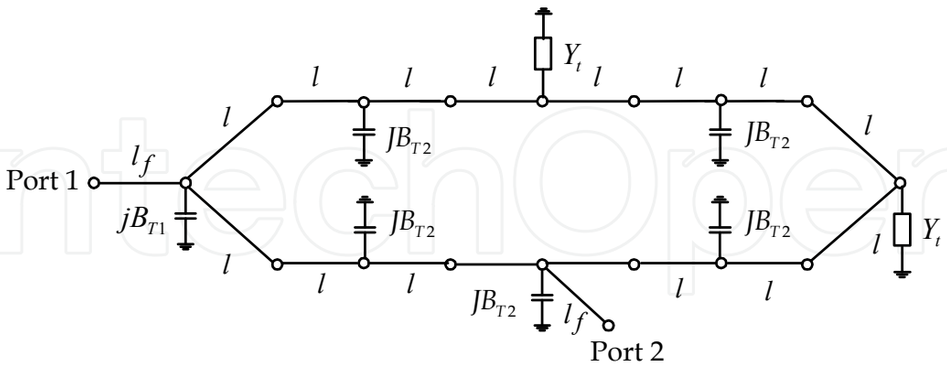

Fig. 17. Equivalent circuit of a microstrip loop resonator with tuning stubs

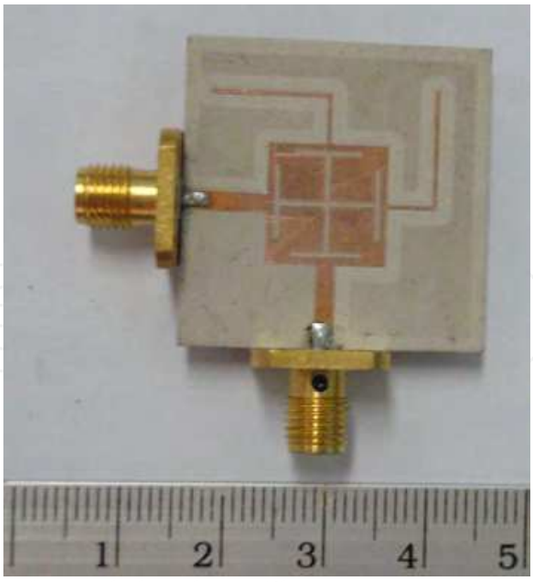

Fig. 18. Photograph of a single-mode bandpass filter

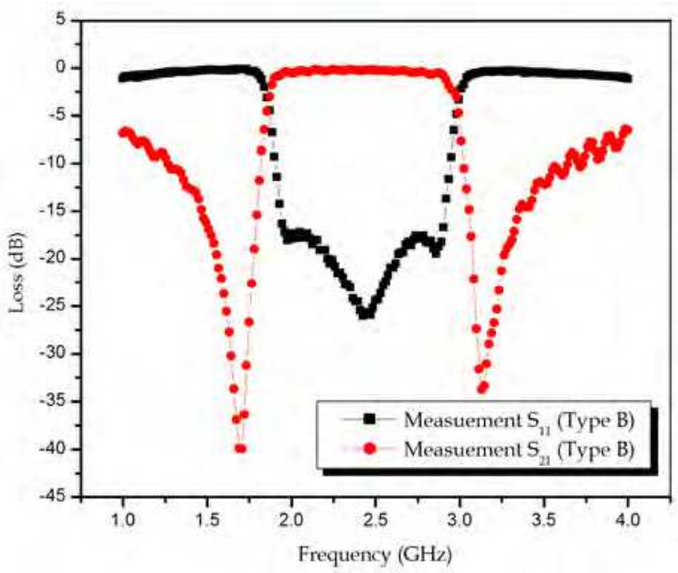

Fig. 19. Measurement for single-mode bandpass filter

Based on bandstop filter. The second resonator is modified by adding two tuning stubs connecting opposite to the ports. The resonator (Type B) with tuning stubs is shown in Fig 16. The length of tuning opened-stub is $l_t = \lambda_g / 4$. The equivalent circuit of resonator with tuning stubs is shown in Fig 17.

The implemented of single-mode resonator filter is pictured in Fig. 18. The measurement results of the microstrip loop with tuning stubs of l_t = 15.35 mm, $w_6 = 0.4$ mm. The frequency response of the filter is portrayed in Fig. 19. The introduction of two tuning stubs connecting opposite to the ports widens the passband and sharpens the stopbands. The

single-mode filter exhibits the 3-dB fractional bandwidth of the filter is 36%, the insertion loss better than 0.19 dB and return loss greater than 17 dB in the passband.

3.3 Dual-mode bandpass filter

3.3.1 Dual-mode bandpass filter (Type A)

By observing the frequency response in Fig. 15, the two stopbands for lower sideband and higher sideband of the filter propose a narrow bandstop. Based on a dual-mode can be used to improve the narrow stopbands.

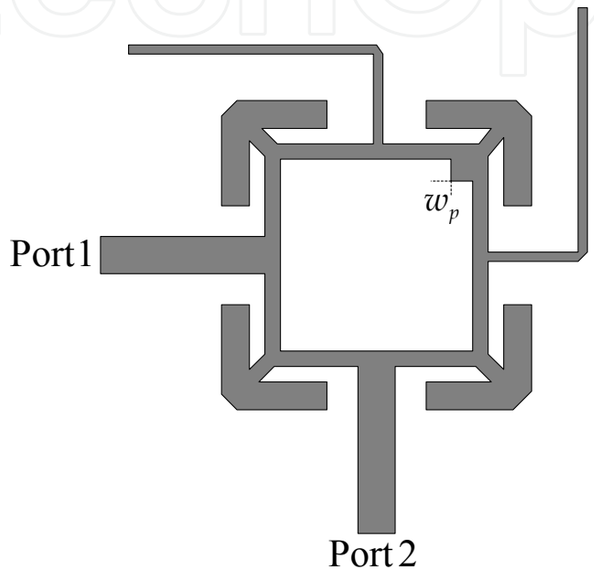

Fig. 20. Structure of dual-mode bandpass filter (Type A)

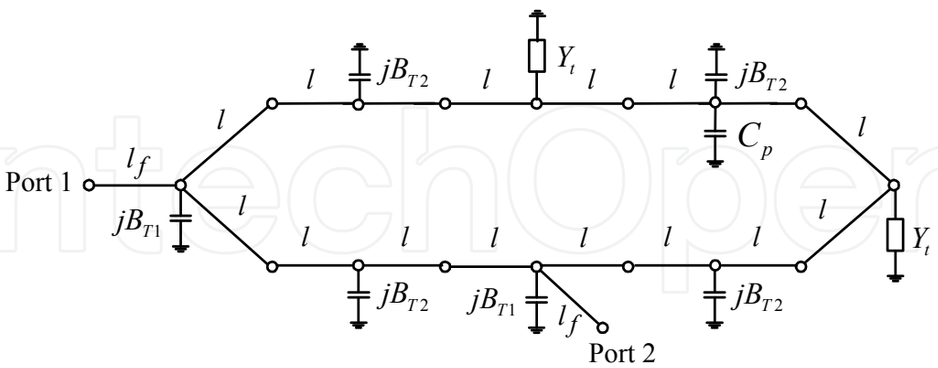

Fig. 21. Equivalent circuit of a dual-mode bandpass filter

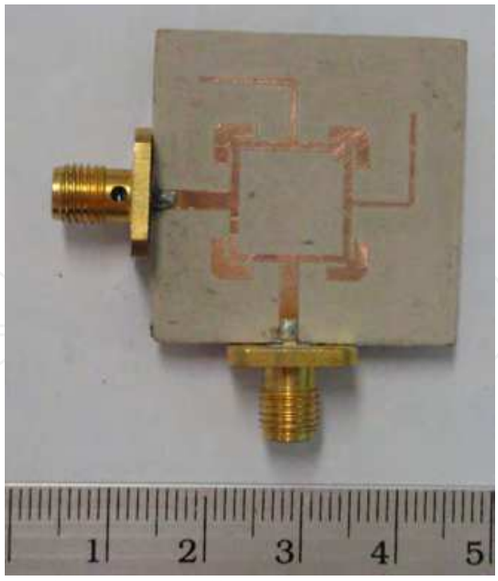

Fig. 22. Photograph of a dual-mode bandpass filter

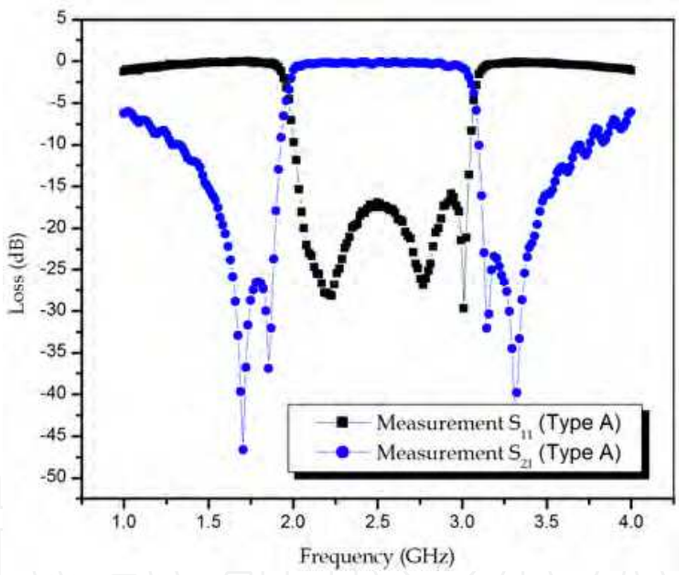

Fig. 23. Measurement of the dual-mode bandpass filter

A square perturbation stub inner corner the loop resonator in Fig. 20. The square stub perturbs the fields of the loop resonator so that the resonator can excite a dual-mode around the stopbands in order to improve the narrow stopbands. By increasing the size of the pertubation stub, the stopband bandwidth between two modes is increaseded. The length of the pertubation stub is $w_p = 1$ mm.

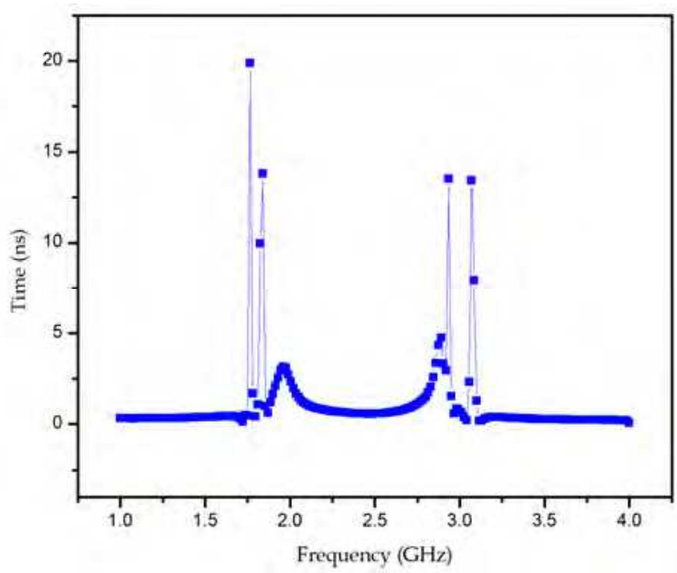

Fig. 24. Measurement group delay of the dual-mode bandpass filter

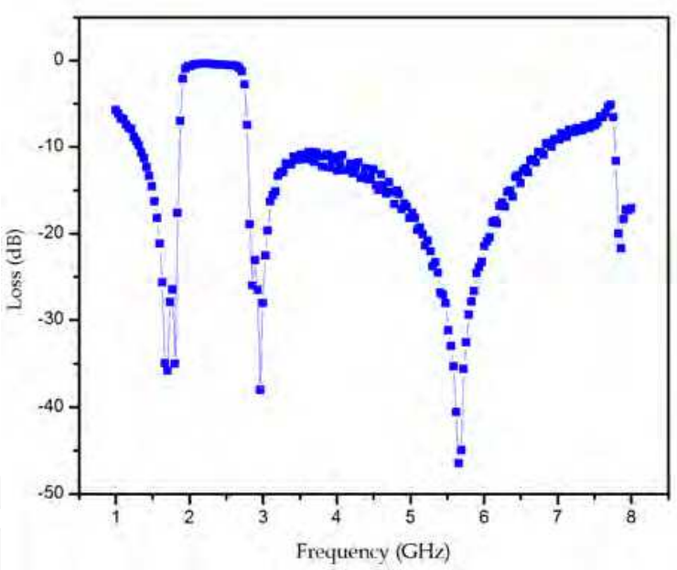

Fig. 25. Measurement wide-band of the dual-mode bandpass filter

Fig.21 delineates the equivalent circuit of the dual-mode bandpass filter (Type A). The asymetric step capacitance C_p can be calculated by

$$C_p = w_p(0.012 + 0.0039\varepsilon_r)\, pF \tag{40}$$

The implemented of dual-mode resonators filter (Type A) is pictured in Fig. 22. The frequency response of the filter is portrayed in Fig. 23. The 3-dB fractional bandwidth of the filter is 36%, the insertion loss is better than 0.34 dB and the return loss is greater than 17 dB in the passband. The group delay of the dual-mode filter can be calculated by

$$\tau = -\partial \frac{\angle S_{21}}{\partial \omega} \tag{41}$$

where $\angle S_{21}$ is the insertion-loss phase and ω is the frequency in radians per second. Fig. 24 shows the group delay of the filter. Within the passband, the group delay is below 2 ns.
The measurement of wide-band response is shown in Fig. 25. Unlike the conventional structure of the wide-band filters using dual-mode ring resonators with tuning stubs, the filter exhibits a wide stopband due to four identical branches at the outer corner of the square loop and proposes the first spurious resonance frequency of the dispersion effect.

3.3.1 Dual-mode bandpass filter (Type B)

By observing the frequency response in Fig. 19, the two stopbands for lower sideband and higher sideband of the filter propose a narrow bandstop. Based on a dual-mode can be used to improve the narrow stopbands.

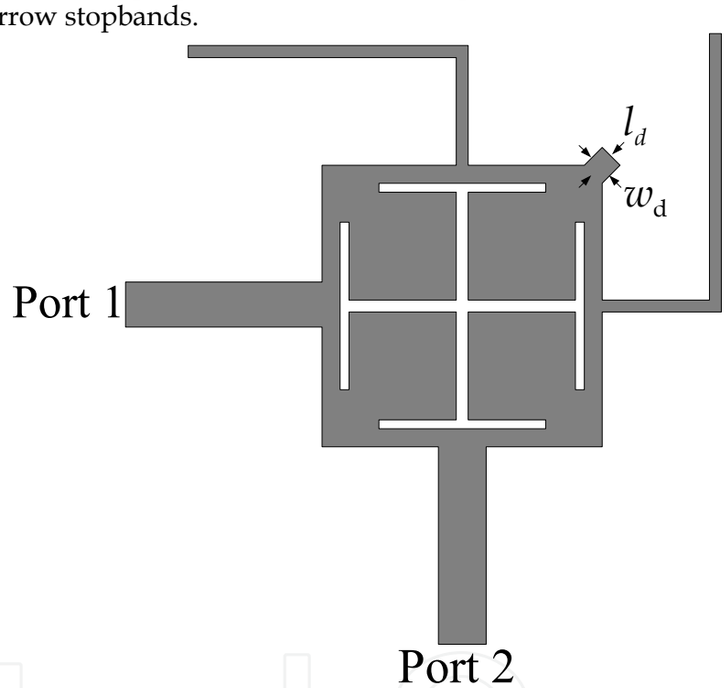

Fig. 26. Structure of dual-mode bandpass filter (Type B)

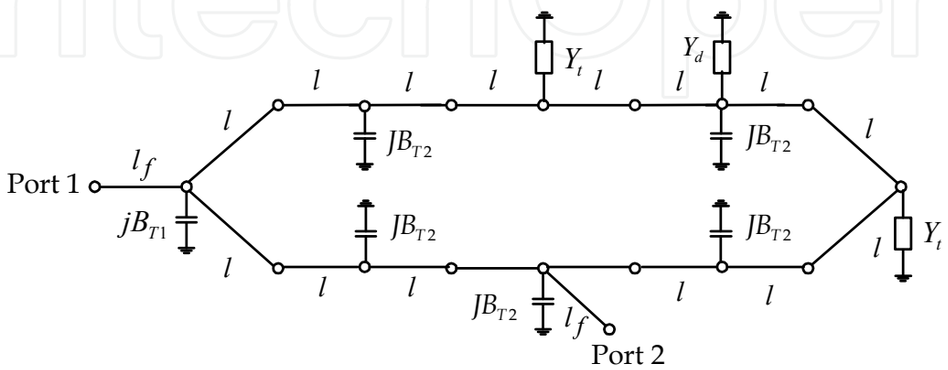

Fig. 27. Equivalent circuit of a dual-mode bandpass filter

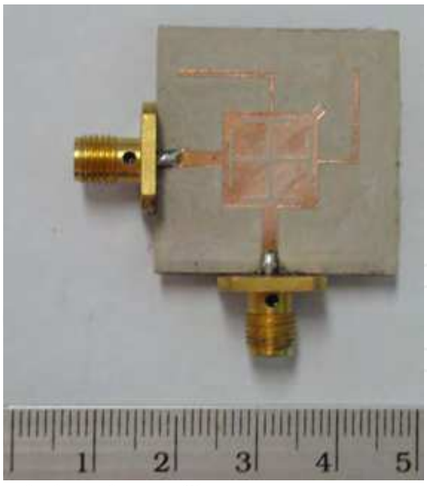

Fig. 28. Photograph of a dual-mode bandpass filter

A square perturbation stub outward corner the loop resonator in Fig. 26. The square stub perturbs the fields of the loop resonator so that the resonator can excite a dual-mode around the stopbands in order to improve the narrow stopbands. By increasing the size of the pertubation stub, the stopband bandwidth between two modes is increaseded. The length of the pertubation stub are w_d = 0.7 mm and l_d = 0.7 mm. Fig.27 delineates the equivalent circuit of the dual-mode bandpass filter. Y_d is the admittance reflecting into the pertubation stub. Y_d can be expressed by

$$Y_d = y_o \tanh(\gamma l_d + l_{open}) + jB_{T3} \tag{42}$$

where y_o is the characteristic admittance of the stub, γ is the complex propagation constant, l_{open} is the equivalent open effect length and jB_{T3} is the capacitance of the junction between the microstrip loop with pertubation stub l_d.

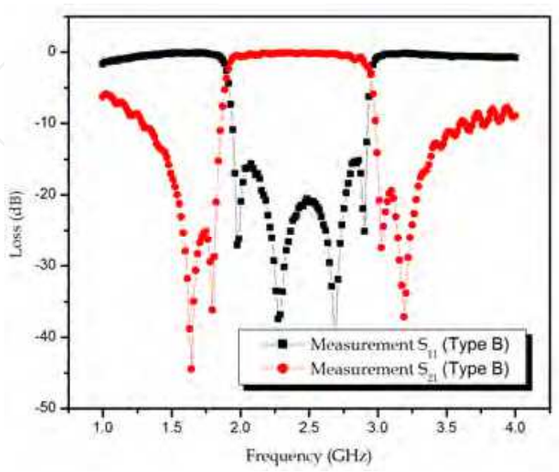

Fig. 29. Measurement of the dual-mode bandpass filter

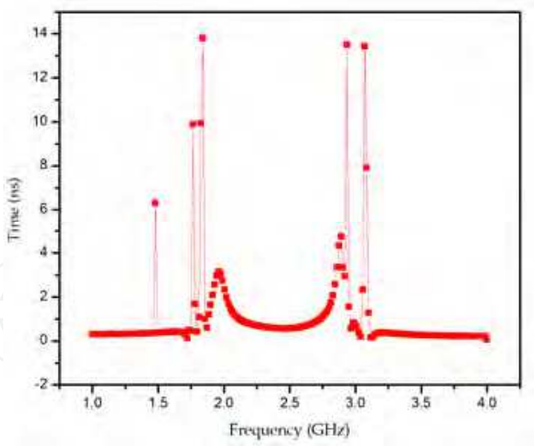

Fig. 30. Measurement group delay of the dual-mode bandpass filter

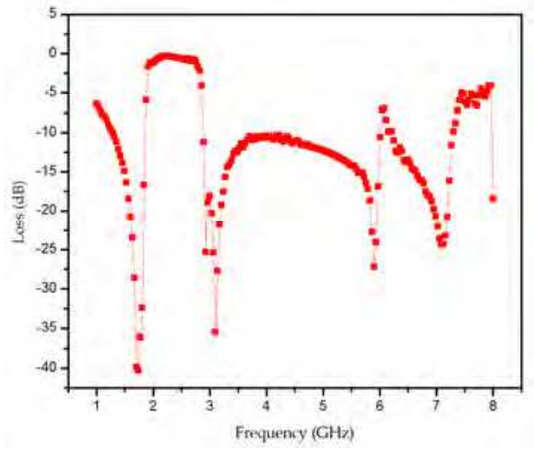

Fig. 31. Measurement wide-band of the dual-mode bandpass filter

The implemented of dual-mode resonators filter is pictured in Fig. 28. The frequency response of the filter is portrayed in Fig. 29. The 3-dB fractional bandwidth of the filter is 36%, the insertion loss is better than 0.15 dB and the return loss is greater than 15 dB in the passband. Fig. 30 shows the group delay of the filter. Within the passband, the group delay is below 2 ns. The measurement of wide-band response is shown in Fig. 31. The filter have a wide stopband resulting from the dispersion effect and the slow-wave effect.

4. Conclusions

In this book, A dual-mode wide-band bandpass filter using the microstrip loop resonators with tuning stubs is proposed here.

4.1 Conclusion

The dual-mode bandpass filter is based on the bandstop filter employing direct-connected feed lines on the orthogonal of the microstrip loop resonators. The introduction of two tuning open stubs connecting opposite to the ports widens the passband and sharpens the stopbands. Then, a dual-mode can be used to improve the narrow stopbands for lower side

band and higher sideband. The filters are designed 2.45 GHz. The 3-dB fractional bandwith of the filter are more than 36%. The group delay of the filter within the passband are below 2 ns. The filters can suppress unwanted passband to below -10 dB.
The first resonator (Type A) consists of four identical branches with attached to an outer corner of the square loop with outer tuning stubs. The filters proposes 0.34 dB insertion loss and return loss greater than 17 dB.
The second resonator (Type B) consists of four identical branches with a small square patch attached to an inner corner of the square loop with outer tuning stubs.The filter proposes 0.15 dB insertion loss and return loss greater than 15 dB.
The both filters (Type A) and (Type B) have a wide stopband resulting from the dispersion effect and the slow-wave effect.

4.2 Problem and suggestion for furure work

There are some problems. The filters can suppress unwanted passband to below -10 dB. On the other hand, the modern wireless communication systems require the bandpass filters having effective out-of-band spurious rejection and good in-band performance. This problem can be overcome by bandstop filter. Microstrip bandstop filter using shunt open stubs and spurlines are presented (Tu & Chang 2005). Basically, by cascading more identical open-stub and spurelines filter, a deeper rejection and a wider rejection bandwidth can be achieved at the expense of increasing circuit size and insertion loss.

5. References

D.M. Pozar (1998). *Microwave Engineering*, 2nd ed. New York: Wiley

Lung-Hwa Hsieh & Kai Chang (2001). Compact, low insertion-loss, sharp-rejection wideband bandpass filters using dual-mode ring resonators with tuning stubs, *Microwave and Optical Technology Letters*, Vol.45, No.4, pp.312-315

Lung-Hwa Hsieh & Kai Chang (2003). Compact,Low Insertion-Loss,Sharp-Rejection and Wide-Band Microstrip Bandpass Filters, *IEEE Transactions on Microwave theory and Techniques*, Vol.51, No.4, pp.1241-1246

Konpang, J. (2003). A Wideband Bandpass Filter Using Square-Loop Resonators with Tuning Stubs, *Master Thesis*, Department of Electrical Engineering, King Mongkut's Institute of Technology North Bangkok

Chu-Yu Chen, Cheng-Ying Hsu & Sung- Fong Lin (2005). A Novel Compact Miniaturiaturized Wideband Microstrip Bandpass Filters with Dual-Mode Ring Resonators, *Microwave and Optical Technology Letters*, Vol.45, No.4, pp.312-315

Jia-sheng Hong & Michael J. Lancaster (1997). Theory and Experiment of Novel Microstrip Slow-Wave Open-Loop Resonator Filters, *IEEE Transactions on Microwave theory and Techniques*, Vol.45, No.12, pp.2358-2365

Adnan Görür (2002). A Novel Dual-Mode Bandpass Filter With Wide Stopband Using the Properties of Microstip Open-Loop Resonator, *IEEE Microwave and Wireless Components Letters*, Vol.12, No.10, pp.386-388

Jia-Sheng Hong & M. J. Lancaster (2001). *Microstrip Filters for RF/Microwave Applications*, New York: John Wiley & Sons, Inc.

K.C. Gupta, R.Garg, I.Bahl & P.Bhartia (1996). *Microstrip Line and Slotlines*, 2nd ed., Artch House

Konpang, J.; Jumneansri, C.; Anunvrapong, P.; & Wongmethanukroah, J.; (2007). A dual-mode wide-band bandpass filter using the microstrip loop resonator with tuning stubs, *Microwave Conference, 2007. European*, pp. 791-794

Konpang, J. (2008). A dual-mode wide-band bandpass filter using slotted patch resonator with tuning stubs, *Microwave Conference, 2008. APMC 2008. Asia-Pacific*, pp.1-4

Wen-Hua Tu & Kai Chang (2005). Compact Microstip Filter Using Open Stub and Spurline, *IEEE Microwave and Wireless Components Letters*, Vol.15, No.4, pp.268-270

IE3D Version *8*, (2001). *Zeland Software*, Inc., Fremont, CA

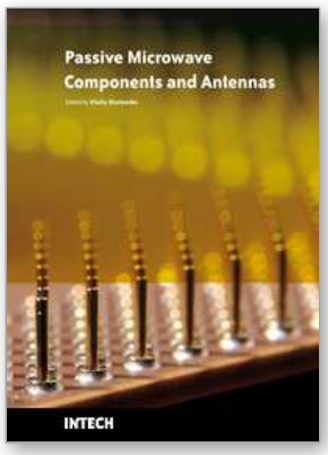

Passive Microwave Components and Antennas

Edited by Vitaliy Zhurbenko

ISBN 978-953-307-083-4
Hard cover, 556 pages
Publisher InTech
Published online 01, April, 2010
Published in print edition April, 2010

Modelling and computations in electromagnetics is a quite fast-growing research area. The recent interest in this field is caused by the increased demand for designing complex microwave components, modeling electromagnetic materials, and rapid increase in computational power for calculation of complex electromagnetic problems. The first part of this book is devoted to the advances in the analysis techniques such as method of moments, finite-difference time- domain method, boundary perturbation theory, Fourier analysis, mode-matching method, and analysis based on circuit theory. These techniques are considered with regard to several challenging technological applications such as those related to electrically large devices, scattering in layered structures, photonic crystals, and artificial materials. The second part of the book deals with waveguides, transmission lines and transitions. This includes microstrip lines (MSL), slot waveguides, substrate integrated waveguides (SIW), vertical transmission lines in multilayer media as well as MSL to SIW and MSL to slot line transitions.

InTech Europe
University Campus STeP Ri
Slavka Krautzeka 83/A
51000 Rijeka, Croatia
Phone: +385 (51) 770 447
Fax: +385 (51) 686 166
www.intechopen.com

InTech China
Unit 405, Office Block, Hotel Equatorial Shanghai
No.65, Yan An Road (West), Shanghai, 200040, China
中国上海市延安西路65号上海国际贵都大饭店办公楼405单元
Phone: +86-21-62489820
Fax: +86-21-62489821

IntechOpen